Predictions and measurements of laminar flow over two-dimensional obstacles

M. G. Carvalho

Instituto Superior Tecnico, Mechanical Engineering Department, Avenido Rovisco Pais, 1096 Lisboa, Portugal

F. Durst and J. C. F. Pereira

Lehrstuhl für Strömungsmechanik, Universität Erlangen-Nürnberg, Egerlandstr. 13, 8520 Erlangen, Federal Republic of Germany

(Received April 1985)

This paper presents numerical predictions of steady, two-dimensional, laminar flow of an incompressible fluid over obstacles mounted in closed channels. Results of the flow predictions are compared with velocity measurements obtained by means of laser–Doppler anemometry.The main objective of this paper was to compare the performance of different numerical schemes employed for the discretization of the convective terms in the differential equations for two-dimensional laminar flow. The upwind, hybrid central/upwind, power law/upwind, quadratic upstream weighted and hybrid central/skewed upwind finite difference schemes were compared with each other and with corresponding experimental data of the velocity field.The flow around two obstacles with different lengths was considered: a thin fence and an obstacle of finite extension in the flow direction. For each of the obstacles, three blockage ratios were investigated. Conclusions are drawn from the six different flow fields predicted with the schemes and it is shown that the quadratic upstream weighted scheme proved to be the most advantageous regarding accuracy against computing time and storage space. For one of the cases investigated, however, this scheme produced 'wiggles' in the solution field.

Keywords: laser-Doppler anemometer, laminar flow, finite differences

There are many ways to classify incompressible fluid flows occuring in various fields of engineering. For computational purposes, it is common to classify flows as:

- *Parabolic flows* fully described by a set of parabolic partial differential equations, the so-called boundary layer equations.
- *Elliptic flows* described by a set of elliptic partial differential equations, and by the continuity and Navier-Stokes equations.

The equations for the former class of flows result from the Navier-Stokes equations by introducing simplifying assumptions. Such assumptions were found necessary in the past to permit flow predictions to be carried out with the reduced computational capabilities that were available and/or were introduced to allow analytical treatments of flows. In recent years, advances in numerical techniques for solutions of partial differential equations (PDEs), together with the development of larger digital computers, have provided a good basis for computing elliptic flows, i.e. to provide numerical solutions to the full set of Navier-Stokes equations. The numerical techniques developed and the digital computers available, however, are not yet developed far enough to yield accurate solutions of flow problems relevant to engineering.

To obtain numerical solutions for such flows with existing computers requires the incorporation of physi-

cal assumptions and the employment of mathematical approximations. Even then, numerical solutions of flow problems can only be provided for simplified flow geometries. For such flow geometries, other workers[1–3] indicated that the accuracy of computed complex flows, e.g. flows with separation, is hindered not only by the validity of the particular physical assumptions employed, but also by the accuracy of the numerical schemes used to discretize the set of governing partial differential equations. These investigations clearly stressed that, for numerical predictions of complex flow fields, a concentration of efforts is required on the development of numerical schemes suitable to reduce the inherent discretization errors present in all first order solution procedures commonly employed these days.

It is generally believed that, with the incorporation of advanced turbulence models, improved numerical solution schemes will allow refined studies of the turbulent, separated flows that are of real interest in many fields of engineering. Much effort has already been invested in improving numerical schemes,[4–6] but only a small amount of work exists comparing predictions with different schemes and directly with experimental results.

Computations of laminar flow over an obstacle were carried out in previous studies, e.g. by Greenspan[7] who provided flow results within his general study of solutions of the Navier-Stokes-equations. Ghia and Davis[8] applied conformal transformations to present solutions to the flow past a semi-infinite obstacle. Other numerical studies exist but only a few provide comparisons of numerical and experimental results.[9] It is this comparison which permits conclusions regarding the numerical accuracy of the flow predictions.

Investigations of turbulent flow over obstacles have been performed experimentally[1,10–12] and a review is provided by Durst and Founti.[13] It was concluded that many numerical schemes for solving the flow over obstacles yield too many numerical errors and, therefore, prevent accurate engineering calculations, irrespective of the validity of the physical assumptions, i.e. the turbulence model, introduced into the solution procedures. Reliable conclusions on the performance of turbulence models to predict turbulent, separated flows are only possible when incorporated into reliable computer codes for flow predictions.

In the present paper, an experimental investigation is described of the flow over a fence carried out using laser–Doppler anemometry (LDA) as a measuring technique. The dependence of the reattachment length on Reynolds number was investigated for three blockage ratios ($S/H = 0.25$, 0.5 and 0.75, where H is the channel height and S the fence height). This study allowed the Reynolds number range of which the laminar flow regime is comprised to be determined. In addition, experimental velocity profiles in the laminar flow regime were obtained for several Reynolds numbers to supply experimental data for comparison with predictions using various numerical schemes. The numerical schemes chosen for comparison were the first order upwind scheme (UDS), the hybrid central/upwind scheme (CUDS),[14] the hybrid power law/upwind scheme (PLDS),[15] the hybrid central/skew upwind scheme (CSUDS),[16] and the quadratic upstream weighted scheme (QUDSC).[6]

In addition to the comparisons between the predictions and measurements of the flow over a fence, the flow over an obstacle of finite dimensions in the flow direction was also investigated. This flow configuration was previously studied experimentally by Gackstatter.[17] For the flow over a fence and over an obstacle, the experimental results showed that the flow complexity increases with increasing blockage ratio (S/H) of the obstacle. This makes the selected flow case an ideal one to study the behaviour of different numerical schemes for flows of increasing complexity.

Experimental investigation

Test section and experimental procedures

The single open end air-driven flow channel employed in the present investigation is shown schematically in *Figure 1*. Its major parts were made of aluminium and all parts of the flow channel were machined to very close tolerances regarding parallelity of walls, surface roughness, corner angles, etc. The flow channel received its air supply through a plenum chamber containing flow straighteners to ensure a well-controlled flow at the exit. The side walls of this channel were made from glass of 1 cm thickness in order to give rigidity to the test section and, at the same time, to facilitate laser–Doppler measurements with forward-scattered light. The air flow into this channel contained scattering particles of 1.5 μm mean diameter provided by a silicon oil particle generator similar to the one described by Cherdron *et al.*[18] Two-dimensional obstacles were able to be mounted inside the channel across the entire width. The dimensions and the most important geometrical parameters of the obstacles employed are given in *Table 1*.

Optical arrangement

The laser–Doppler anemometer employed in the present investigation was operated in the so-called fringe mode and was set up to operate with forward-scattered light and to measure only the x-velocity component, which is in the flow direction and parallel to the channel walls. The optical system consisted of a 15 mW Ne–He laser, an integrated LDA optical system, manufactured by OEI-Opto-Elektronische Instrumente, and incorporating double Bragg cells, light collecting optics and a photomultiplier. A transient recorder was used to digitize and store the signals from the high-pass filtered output of the photomultiplier. These signals were then transferred to a Hewlett Packard computer (HP A700) and processed as described by Durst and Tropea.[19] For a given measurement of local, time-mean velocity at a known x-y position, 100–5000 Doppler bursts were processed and averaged, each having at least 50 signal cycles.

The transient recorder employed was externally triggered at a rate much slower than that at which the Doppler bursts occur in order to eliminate biasing for time-varying flow conditions. A time of 1–5 min, depending on the status of the flow and the location in the flow field, was needed for each measuring point to gather and process the required number of Doppler bursts.

Experimental results

Measurements of the reattachment length and velocity distribution of the flow over a fence were carried out

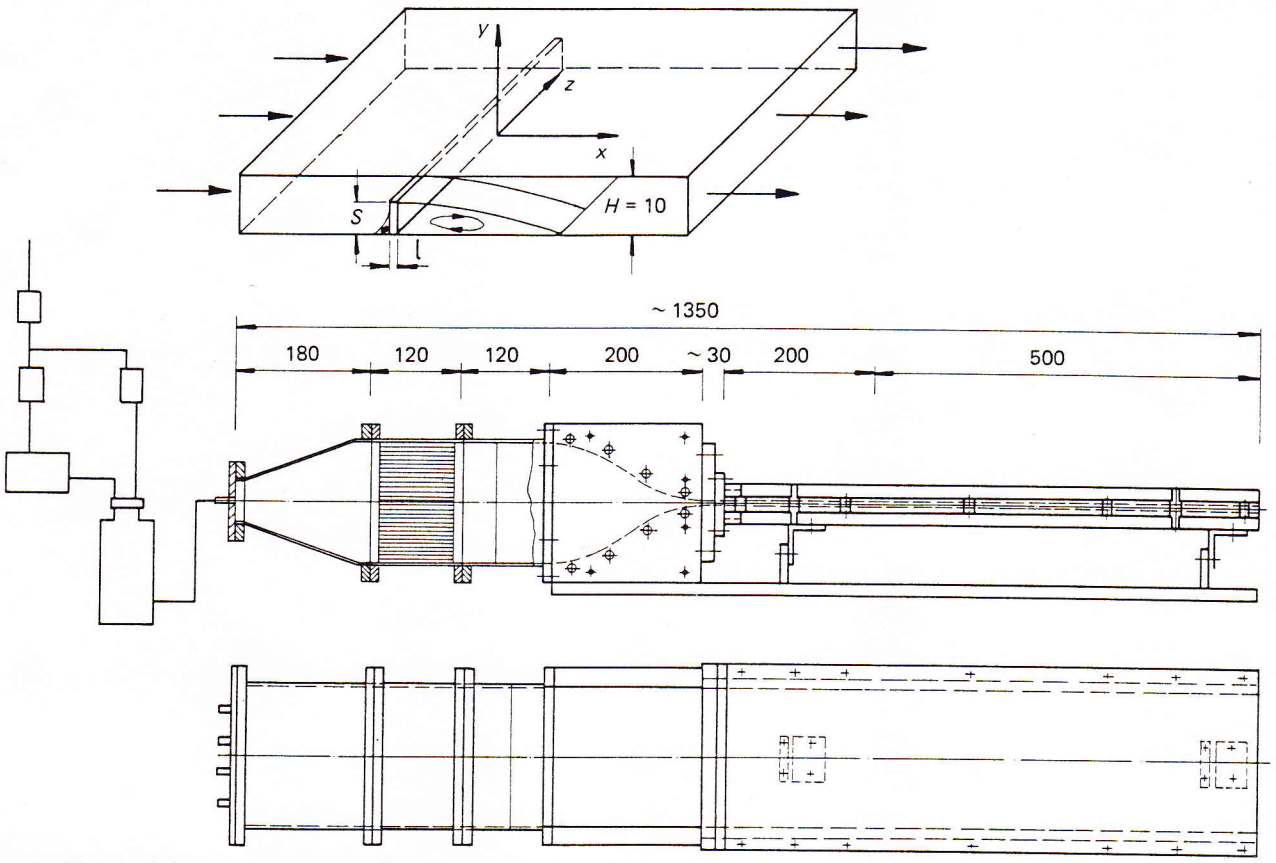

Figure 1 Sketch of air tunnel and test section (dimensions in mm)

Table 1 Test section dimensions

Test section dimensions	H (mm)	L (mm)	h (mm)	S (mm)	S/H	L/H
			7.5	2.5	0.75	
Obstacle	10	180	5	5	0.50	18
			2.5	7.5	0.25	

with the instrumentation described above and are presented here for channel Reynolds numbers in the range $50 \leq Re_S \leq 2000$ and for channel blockage ratios (S/H of 0.25; 0.5 and 0.75). The definition of the Reynolds number used in this study is given by:

$$Re_S = \frac{\tilde{U} \cdot S}{\nu} \qquad (1)$$

where $\tilde{U}$ is the cross-sectional average inlet channel velocity, corresponding, in the laminar regime, to two-thirds of the maximum channel velocity. S is the obstacle height and ν the kinetic viscosity. The choice of length scale to base the Reynolds number on is somewhat arbitrary, but experience has shown that the variations in reattachment length, X/S, for different blockage ratios, S/H, are well correlated with Re_S.

The first set of measurement results concerns the lengths of the primary and secondary recirculation regions occuring after the fence. They are dependent on the flow Reynolds number and obstacle blockage ratio, as well as the obstacle extension in the flow direction.

The dependence of the length of the primary recirculation zone, X_1 on Reynolds number, as shown in *Figure 2*, follows the general behaviour also common to the backward-facing step flow.[20] Three flow regimes can be

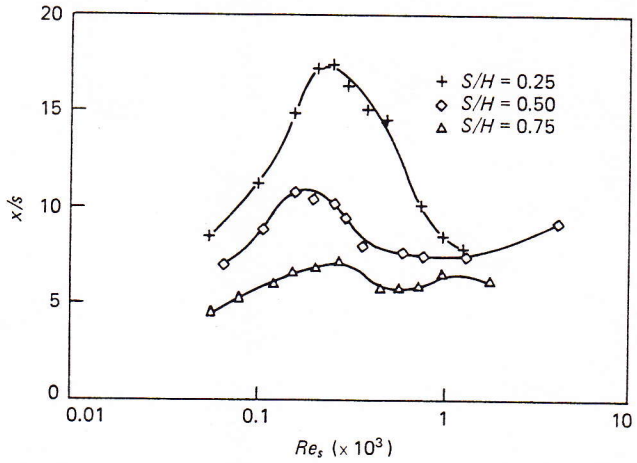

Figure 2 Dependence of length of primary recirculation zone on Reynolds number: *1* = 1 mm

identified from the variation of separation length: a laminar regime with a steady increase in X_1/S with Reynolds number up to $Re_S \sim 250$; a transitional regime marked by a steady decrease in X_1/S within $250 \leq Re_S \leq 1500$; and a partial separation length recovery into what would finally become the turbulent regime in which X_1/S is not expected to vary much with Reynolds number. The existing flow range limitations of the present test rig did not allow the study of the turbulent flow regime. To the authors' knowledge, however, the presented measurements of reattachment length variation with Reynolds number that cover the laminar and transitional regimes of flow over a fence with laser–Dopler anemometry are the first of their kind.

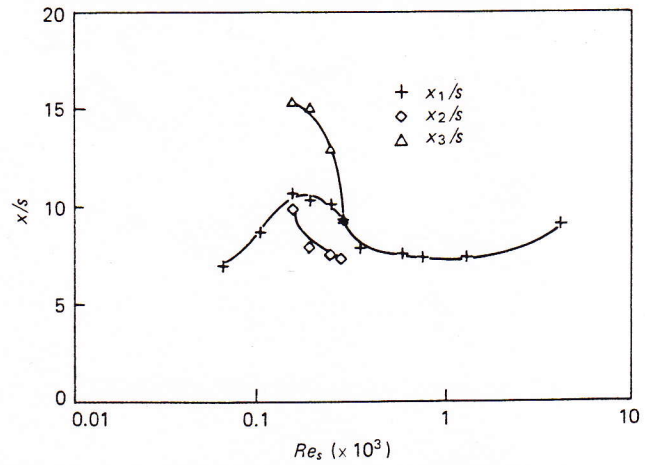

Figure 3 Reattachment lengths as function of Reynolds number for fence: $S/H = 0.5$; $1 = 1$ mm

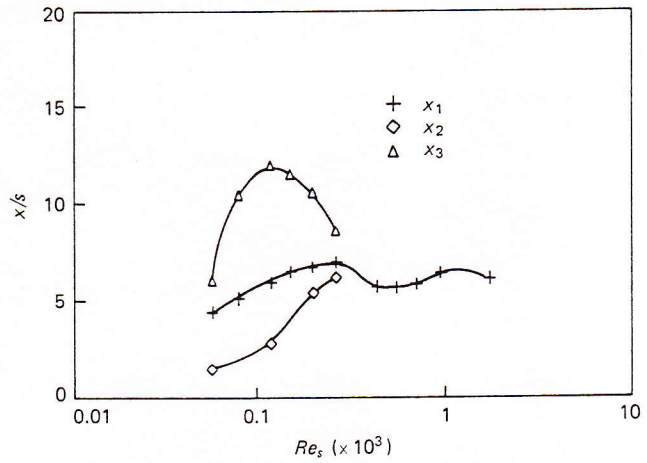

Figure 4 Reattachment lengths as function of Reynolds number for fence: $S/H = 0.75$; $1 = 1$ mm

Figure 2 already shows the effect of the blockage ratio on the separation length X_1/S for the fence geometry. Strictly speaking, the block length-to-step height ratio l/S has also been varied in this diagram, but from previous results[21] this should have little influence at least for the range of l/S in question. It can be seen from *Figure 2* that the reattachment length drops significantly with increasing blockage of the channel for the laminar and transitional flow conditions investigated here. Although the turbulent range has not been investigated, the influence is expected to be somewhat weakened in that flow regime.

One reason for the very marked changes of X_1/S with blockage ratio is undoubtedly the appearance of a secondary recirculation zone on the wall opposite the fence. Details of this reverse flow region can be seen in *Figures 3* and *4* for the fences with $S/H = 0.5$ and $S/H = 0.75$, respectively. No such secondary separated flow region was found for the fence with $S/H = 0.25$. Although the interaction between the pressure field and the velocity field is not fully understood in regions of flow separation, it is evident that the recirculation zone in *Figures 3* and *4* is a result of a strong adverse pressure gradient due to the sudden expansion behind the fence. Since the flow acceleration is considerably greater for the fence with blockage ratio $S/H = 0.75$, it is not surprising that this recirculation zone is already found at lower values of Reynolds number, as can be seen by comparing *Figures 3* and *4*.

In addition to the general investigations of the flow structure, i.e. the measurement of the integral parameters, detailed velocity profiles were obtained for Reynolds numbers in the laminar flow regime. *Figure 5* shows, as an example, the U-velocity profiles at several X/S locations for the fence with blockage ratio $S/H = 0.5$. The two regions of recirculating fluid, one attached to the bottom channel wall after the obstacle and the other to the top channel wall can be clearly distinguished.

Governing flow equations and solution procedure

Governing equations

The partial differential equations (PDE) governing the steady recirculating flows presented in this study are the Navier-Stokes equations. Mass conservation also holds and this can be formulated to yield the continuity equation. The flows considered are two-dimensional and incompressible and, hence, the general PDEs describing the flow field are:

Continuity equation:

$$\frac{\partial \rho U}{\partial x} + \frac{\partial \rho V}{\partial y} = 0 \tag{2}$$

Momentum equations:

$$\frac{\partial \rho UU}{\partial x} + \frac{\partial \rho VU}{\partial y} = -\frac{\partial p}{\partial x} + \mu\left(\frac{\partial^2 U}{\partial x^2} + \frac{\partial^2 U}{\partial y^2}\right) + S_u \tag{3}$$

$$\frac{\partial \rho UV}{\partial x} + \frac{\partial \rho VV}{\partial y} = -\frac{\partial p}{\partial x} + \mu\left(\frac{\partial^2 V}{\partial x^2} + \frac{\partial^2 V}{\partial y^2}\right) + S_v \tag{4}$$

These equations can be written in the form of a general transport equation, as follows:

$$\frac{\partial \rho U\phi}{\partial x} + \frac{\partial \rho V\phi}{\partial y} = \mu\left(\frac{\partial^2 \phi}{\partial x^2} + \frac{\partial^2 \phi}{\partial y^2}\right) + S_\phi \tag{5}$$

where ϕ denotes the U or V velocity components and S_ϕ represents the pressure gradient term in the x- and y-directions. The continuity equation results from this general transport equation by setting $\phi = 1$ and $S_\phi = 0$.

The transformation of the PDEs for the U- and V-momentum into the equivalent finite difference equations (FDEs) can be obtained by using the finite volume method.[22] The application of the finite volume method requires discretizations of the convective and diffusive fluxes at each control volume face. In the present study,

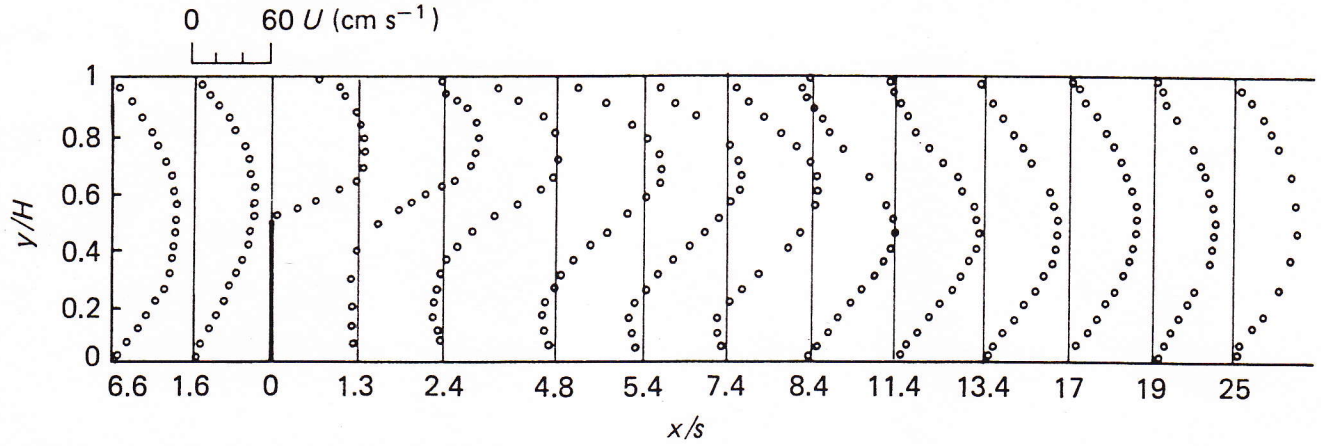

Figure 5 *U*-velocity profiles for fence: $S/H = 0.5$; $Re_s = 112$

the diffusive fluxes were always approximated by central differences known to be of third order accuracy.

Numerical schemes for discretization of convective terms

The approximation of the convective fluxes in the momentum equations applied at each control volume face was performed with different numerical schemes. Five numerical schemes were used:

- The upwind differencing scheme (UDS) is the simplest unconditional stable scheme to approximate the convection terms. It, however, induces a truncation error which is felt like a diffusive term in the equations. This can lead to low accuracy in predicted solutions of flow fields. This discretization scheme approximates the ϕ-control volume face value by the nodal value taken in the upstream direction of the velocity.
- The hybrid central/upwind differencing scheme (CUDS) is based on the exact solution of the linear one-dimensional steady convection–diffusion equation between any two neighbouring mesh nodes.[14] The convective terms are approximated by central differences for Peclet numbers ($Pe = \rho\Delta U/\Gamma$), $|Pe| < 2$. For $|Pe| > 2$, the convection terms are approximated by UDS.
- The hybrid power law/upwind differencing scheme (PLDS), in comparison to the above schemes, represents a better approximation of the exact solution of the one-dimensional convection–diffusion equation. In this approximation,[15] a 'power law' is used for $|Pe| < 10$ and UDS for $|Pe| > 10$.
- The hybrid central/skew upwind differencing scheme (CSUDS)[16] strongly reduces the problem caused by the flow direction to grid line skewness. For Peclet number $|Pe| > 2$, this scheme tries to simulate a grid in which the coordinate grid lines are aligned with the local flow direction. It takes explicit account of the local flow angle by determining the velocity vector tangential to the streamline at the control volume face. For $|Pe| < 2$, the scheme uses central differences for the discretization of the convection terms in the equations.
- The quadratic weighted upstream differencing scheme (QUDSC)[6] is based on a local quadratic interpolation at the ϕ-surface for estimating both the convective and diffusive flux terms on each control volume face individually. For non-uniform grid distributions the local quadratic interpolations were derived taking into account the non-uniformity between mesh points.[23]

Solution procedure

All computations presented in this paper were performed with an appropriately modified version of the computer code TEACH[22] designed to solve two-dimensional elliptic flow problems in terms of the primitive hydrodynamic variables U, V and P. The code, in its original form, uses CUDS and is based on the so-called SIMPLE solution algorithm of Patankar and Spalding[15] for the solution of the final set of linear equations. As a first step in solving a specified flow problem, the TEACH program computes a preliminary velocity field by solving discretized versions of the momentum equations employing a guessed pressure field. This field is then improved by solving the pressure-correction equation which contains a dilatation term (i.e. the local mass imbalance) as a source. In the present study, the system of algebraic equations resulting from the pressure-correction equations was always solved by the 'strongly implicit method'[24] instead of the tri-diagonal matrix algorithm used for U and V discretized versions of the momentum equations. The reason for using the strongly implicit method for the pressure-correction equation was due to the faster convergence achieved by the strongly implicit method for well-conditioned matrices, as in the case of the pressure correction equation.[25] For the present study, the finite difference discretizations described were incorporated into the computer code TEACH and subsequently used to predict flows over obstacles. Details of the final program are described by Pereira.[26]

Comparison between numerical and experimental results

The flow configuration of interest in this study is depicted in *Figure 6*. Fluid enters from the left-hand side of the channel test section and flows through a parallel plate channel of height H. It then flows over the obstacle of height S and length l leaving the channel at distance l_2 from the obstacle. In the present work, the distances between the inlet plane and the obstacle l_1, exceeded those recommended by Zeisel[27] and Denis

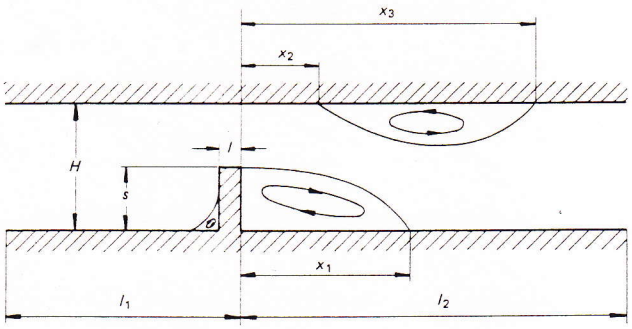

Figure 6 Geometry of flow over fence or obstacle

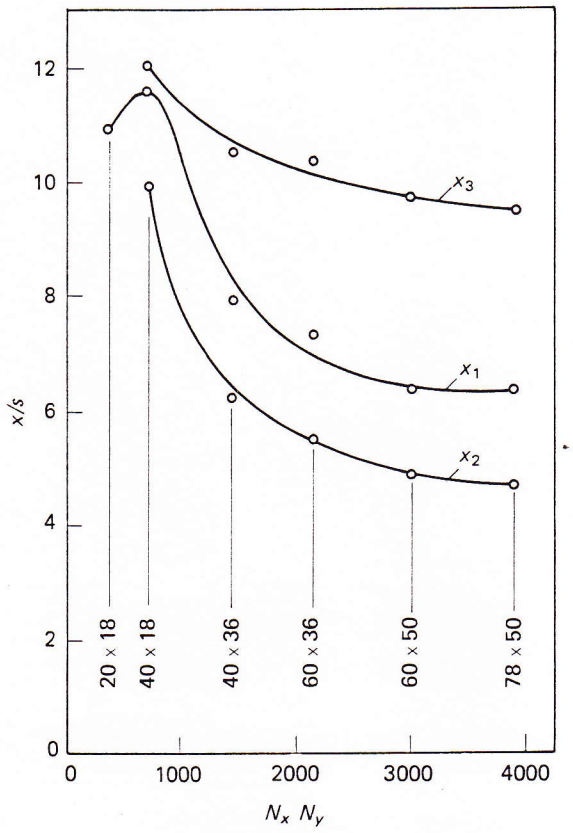

Figure 7 Grid dependence study with CUDS for flow over fence: $S/H = 0.5$; $Re_s = 145$

and Smith[28] in order to obtain a fully-developed velocity profile in the channel before reaching the obstacle. The outlet plane of the channel investigated was located downstream of the obstacle and far enough upstream to ensure a fully developed velocity profile for all flows at the channel outlet. The velocity boundary conditions at the solid walls were those of zero tangential and normal velocities. At the inlet to the channel, a fully-developed laminar U-velocity profile was prescribed and the cross-flow velocity V was set to zero. The boundary conditions at the outlet were $\partial U/\partial x = 0$ and $\partial V/\partial x = 0$.

A grid dependence study of the predicted flow field was performed for the flow over a fence with a blockage ratio $S/H = 0.5$. *Figure 7* shows the reattachment lengths predicted with the CUDS version of the TEACH program and a Reynolds number of $Re = 145$ using six different numerical grids. As can be concluded from *Figure 7*, the grids comprising 60×50 and 78×50 grid

Table 2 Characteristics of flow geometry: flow over fence

Case	H (mm)	l (mm)	S (mm)	l/S	S/H	l_1/S	l_2/S	$Re_S = \bar{U}S/\nu$
I	10	1	2.5	0.4	0.25	20	31	102
II	10	1	5	0.2	0.5	10	43	145
III	10	1	7.5	0.133	0.75	10	40	82.5

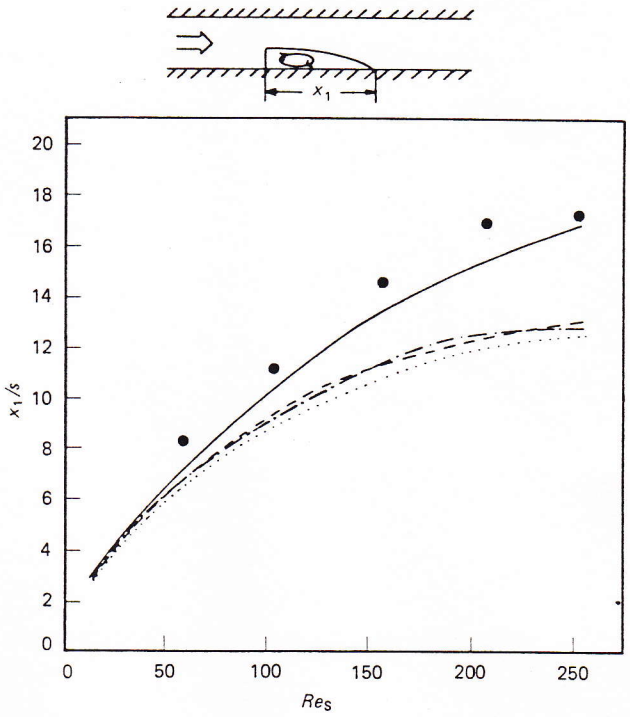

Figure 8 Comparison of reattachment lengths as predicted and measured functions of Reynolds number: (●) measurements; (——) QUDSC; (– – –) PLDS; (– · –) CUDS; (· · · ·) UDS

points show very small differences in the predicted reattachment lengths. This does not mean, however, that grid-independent solutions were obtained. Solutions can be rather sluggish in reaching grid independence and only with a grid of, for example, 150×100 could such conclusion be derived. Due to storage limitations imposed by the available CDC-285 computer, a grid of 60×50 was used and was spread over the flow domain of the six geometries investigated. The numerical grid employed contracted before the obstacle with a contraction ratio of 1.2 and expanded after the obstacle with an expansion ratio of 1.2. In the y-coordinate direction, a high concentration of grid nodes was located around the obstacle top face in order to assure that the high velocity gradients in that region were resolved properly in the flow computations.

Flow over a fence

The three flow configurations investigated for flows over a fence are listed in *Table 2*. For the first flow case, a fence-to-channel height of $S/H = 0.25$ was chosen. *Figure 8* shows the dependence of the reattachment lengths on the Reynolds number of the oncoming flow for the range $Re_S = 12.5$–250. For this flow case, four numerical schemes were compared with each other and with the measurements. The PLDS and CUDS finite difference schemes yielded very similar results. The first

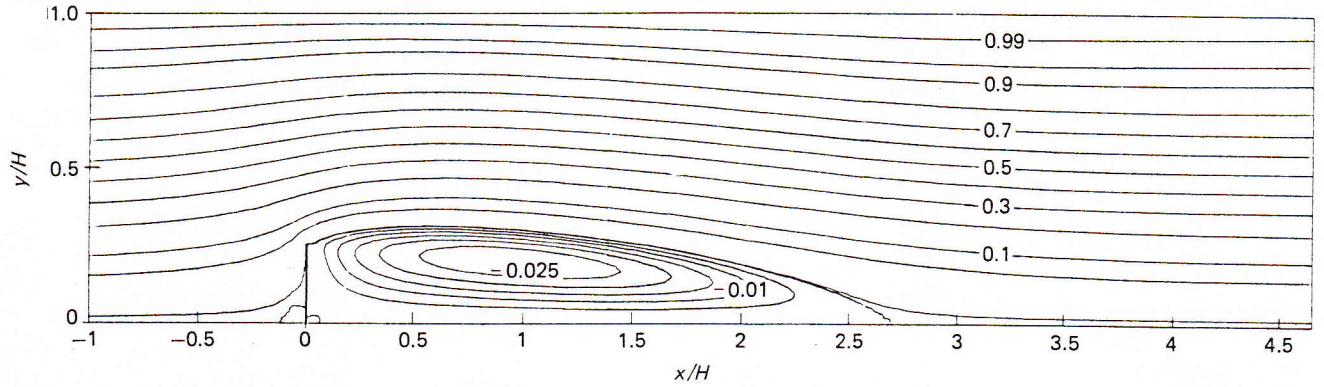

Figure 9 Calculated streamlines with QUDSC scheme for flow over fence: $S/H = 0.25$; $Re_s = 102$

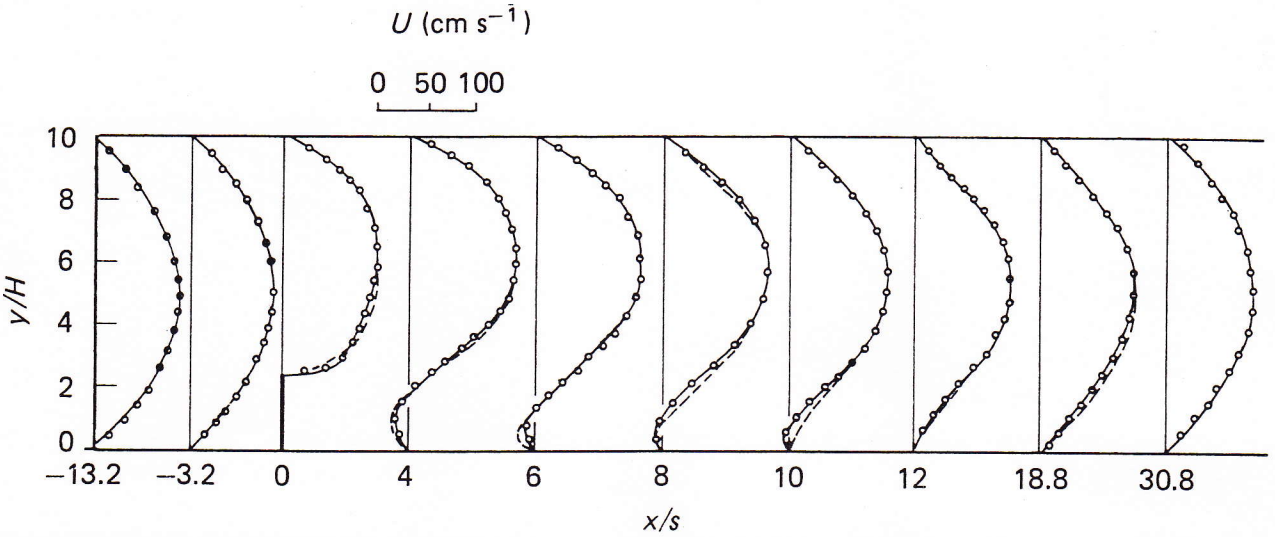

Figure 10 Comparison between predictions and measurements for flow over fence: $S/H = 0.25$; $Re_s = 102$; (——) OUDS; (– – –) CUDS

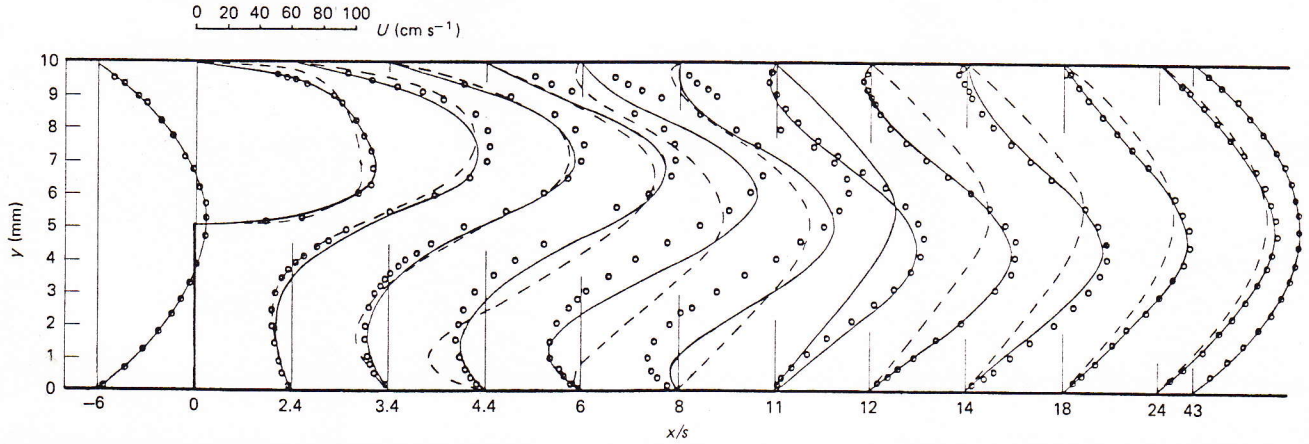

Figure 11 Comparison between predictions and measurements for flow over fence: $S/H = 0.5$; $Re_s = 145$; (——) QUDSC (32 × 35); (– – –) CUDS (60 × 50)

order upwind scheme UDS showed the most unsatisfactory results. The QUDSC scheme resulted in numerical results similar to the measured reattachment values, with a small but consistent lower value. *Figure 9* shows the streamlines calculated with the QUDSC discretization scheme for $Re_S = 102$. The small curvature of the streamlines outside the recirculation region produces a small degree skewness of the velocity vector with the grid lines. This leads to small truncation errors (false diffusion) in the results obtained and it is likely that it is this numerically-caused false diffusion that yields the predicted shorter separation length.

Figure 10 presents the U-velocity profiles at different X/S locations measured and calculated with the QUDSC and CUDS schemes and shows that the main differences are confined to the recirculation region. As the CUDS scheme predicted a smaller length of the recirculation region X_1/S, (see *Figure 8*), the flow recovery is also in observable disagreement with the measurements. The differences in the redevelopment region of

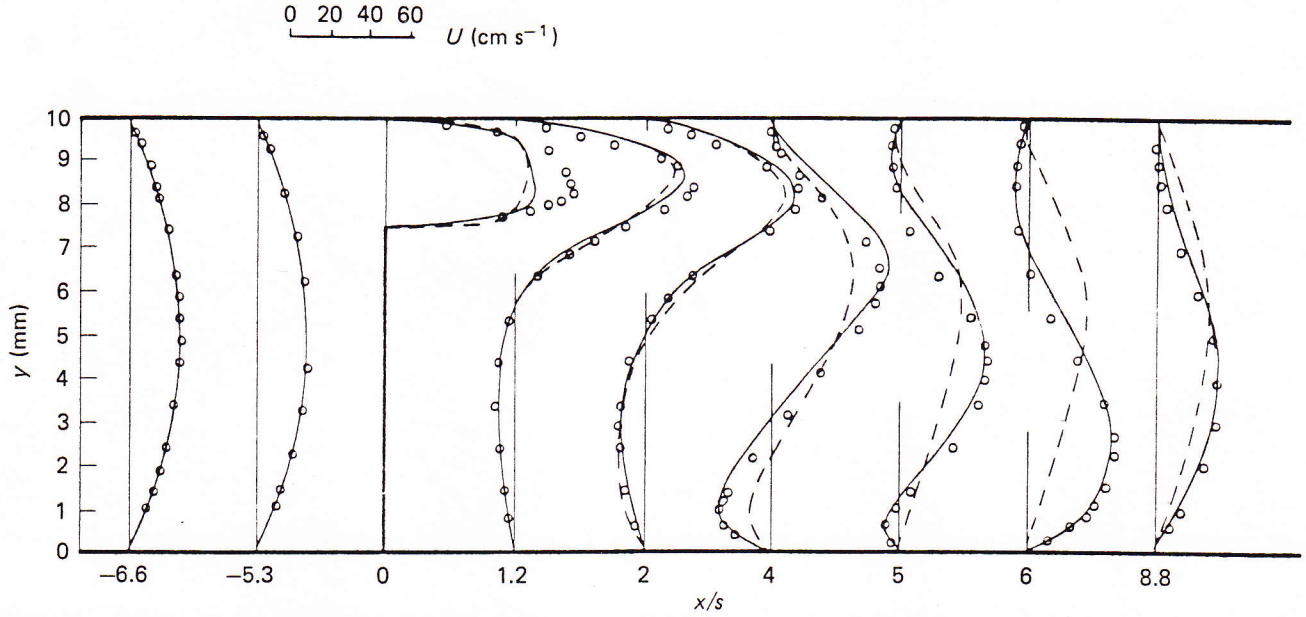

Figure 12 Comparison between predictions and measurements for flow over fence: $S/H = 0.75$; $Re_s = 82.5$; (---) UDS (60 × 50); (——) QUDSC (60 × 50)

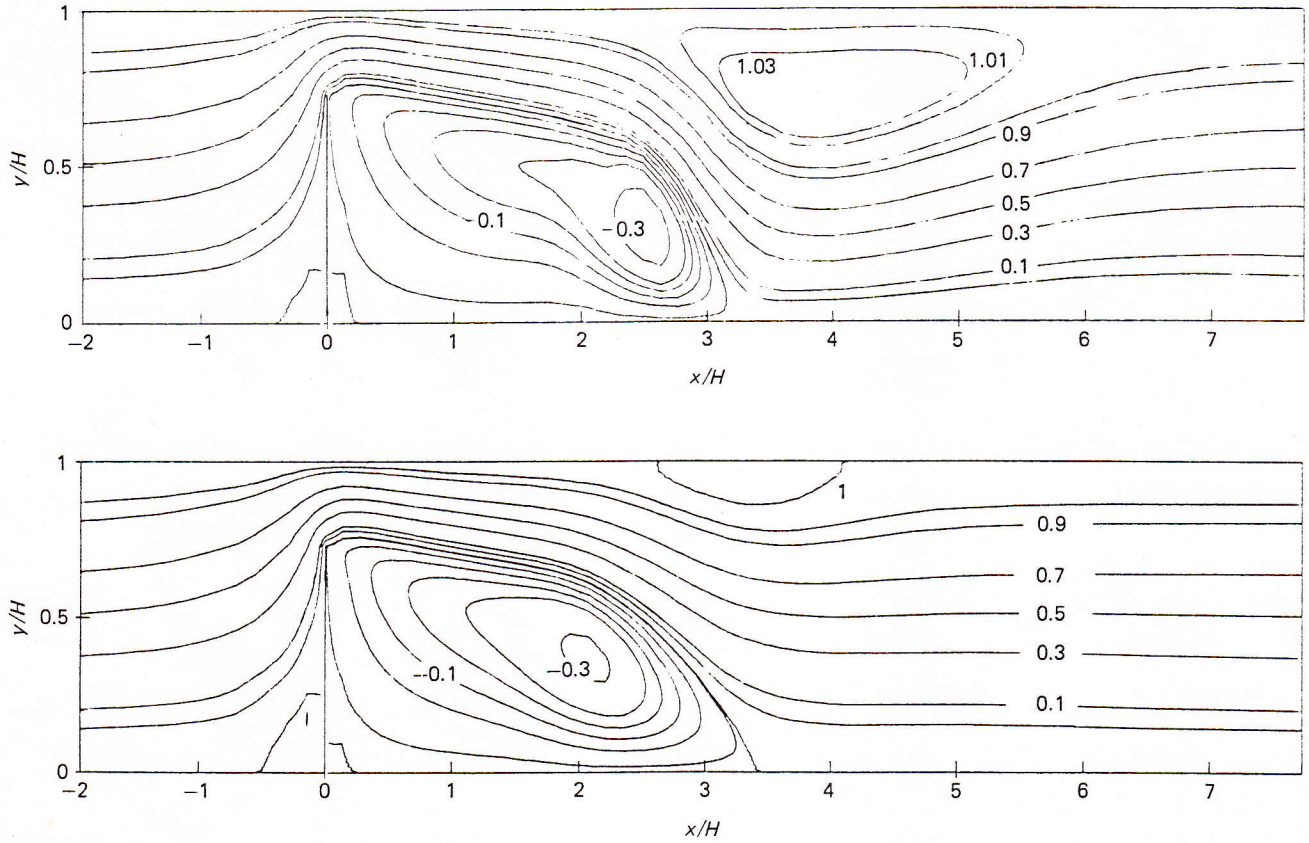

Figure 13

Table 3 Characteristics of flow geometry: flow over obstacle

Case	H (mm)	l (mm)	S (mm)	l/S	S/H	l_1/S	l_2/S	$Re_S = \bar{U}S/\nu$
IV	10	20	2.5	8	0.25	28	20	37
V	10	20	5	4	0.5	14	30	96
VI	10	20	7.5	2.66	0.75	13	40	177

the flow are small, and are expected to result entirely from the deviations of the predicted flow field from the measured velocity field in the vicinity of the recirculating flow region, as shown in *Figure 8*.

Figure 11 shows the comparison of the U-velocity profiles at different X/S stations calculated and measured for the second flow case investigated in this study, (see *Table 2*). It corresponds to flow over a fence with a

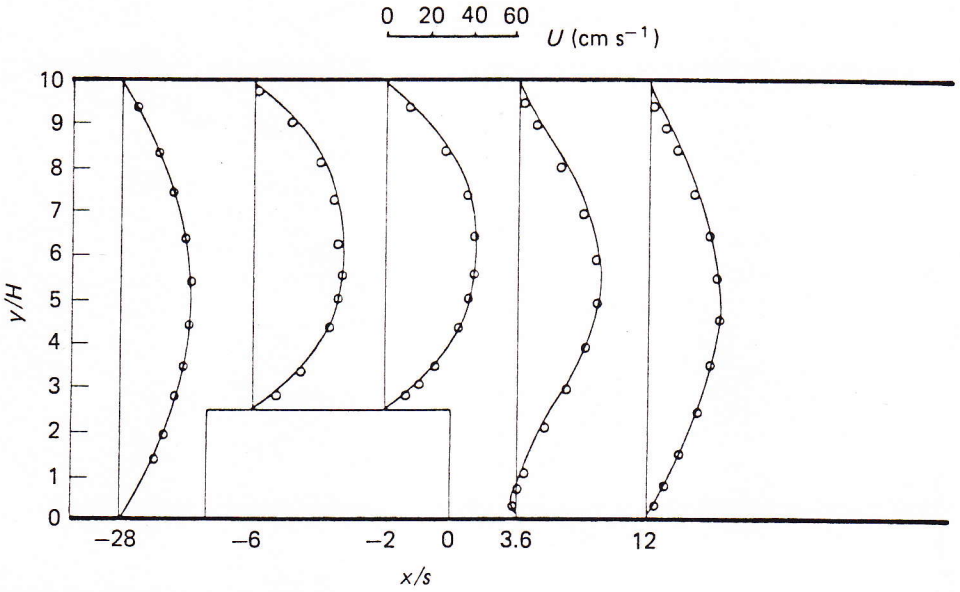

Figure 14 Comparison between predictions and measurements for flow over obstacle: $S/H = 0.25$; $Re_s = 37$; (– – –) OUDSC (57 × 51); (——) CSUDS (57 × 51)

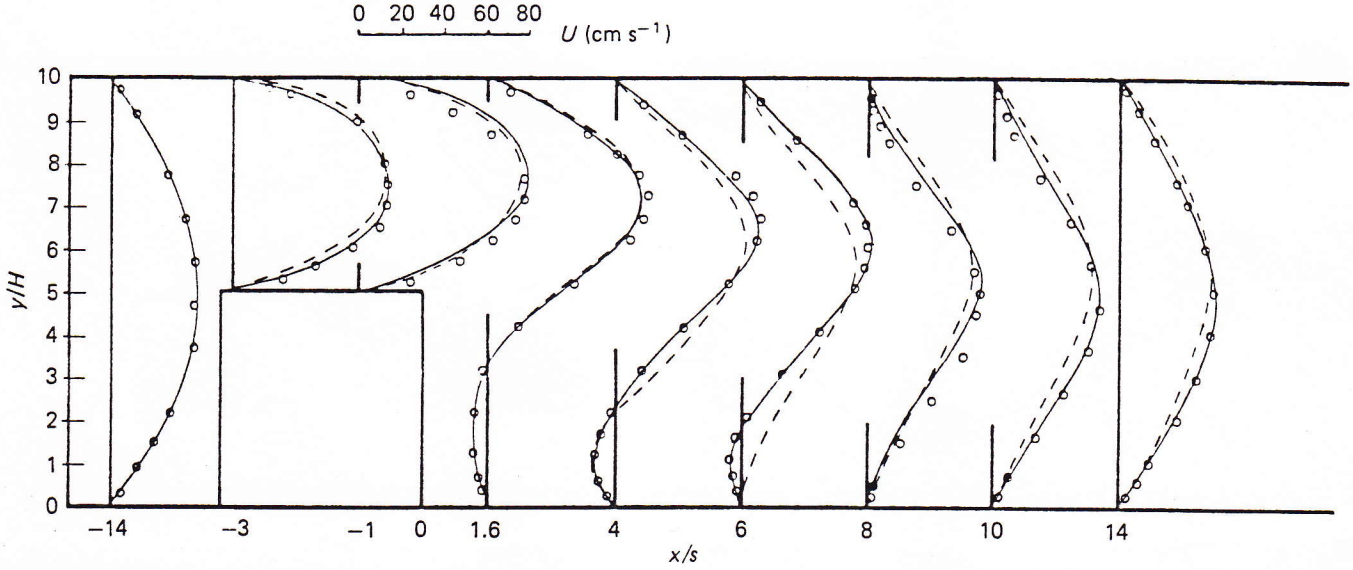

Figure 15 Comparison between predictions and measurements for flow over obstacle: $S/H = 0.5$; $Re_s = 96$; (——) QUDSC (50 × 49); (– – –) PLDS (50 × 49)

fence-to-channel height ratio of $S/H = 0.5$ and a Reynolds number of $Re_S = 145$. *Figure 11* confirms that the CUDS finite difference scheme leads to unsatisfactory results compared with the measurements. Better results are obtained with the QUDSC scheme but, even for this prediction scheme, much smaller numerical grid spacings are necessary to yield closer agreement between measurements and predictions.

Among the cases considered in the present study, the flow over a fence with blockage ratio $S/H = 0.75$ and $Re_S = 82.5$ (*Table 2*) is the most severe test reported here for the various numerical schemes. The flow field displays a high degree of skewness in front of the fence and a large region of high velocity gradients in the shear layer around the recirculation region attached to the fence and located behind it. In addition, a region of high adverse pressure gradient appears on the top channel wall, leading to flow separation on the wall opposite the fence, causing a large recirculation region on the top wall of the channel. Studying this flow case, the choice of the first order upwind UDS scheme for discretization of the convective terms was incorporated into the present study to illustrate the bad performance of a pure first order upwind scheme at low Reynolds numbers. Its behaviour is similar to the behaviour of the hybrid CUDS scheme for high Reynolds numbers.

Figure 12 shows the experimental values of the U-velocity at different X/S locations and the computational results obtained with the UDS and QUDSC schemes. The predictions obtained with the QUDSC scheme are in good agreement with the experimental values. As a consequence of false diffusion, the recirculating flow region on the top wall of the channel predicted by the UDS scheme is much shorter than the corresponding region predicted with the QUDSC scheme. Thus, the recirculation region attached to the fence grows longer for the UDS scheme. The velocity profiles predicted by the UDS scheme for $X/S \approx 4$, however, are in reasonable agreement both with QUDSC and with the measurements. A somewhat observable

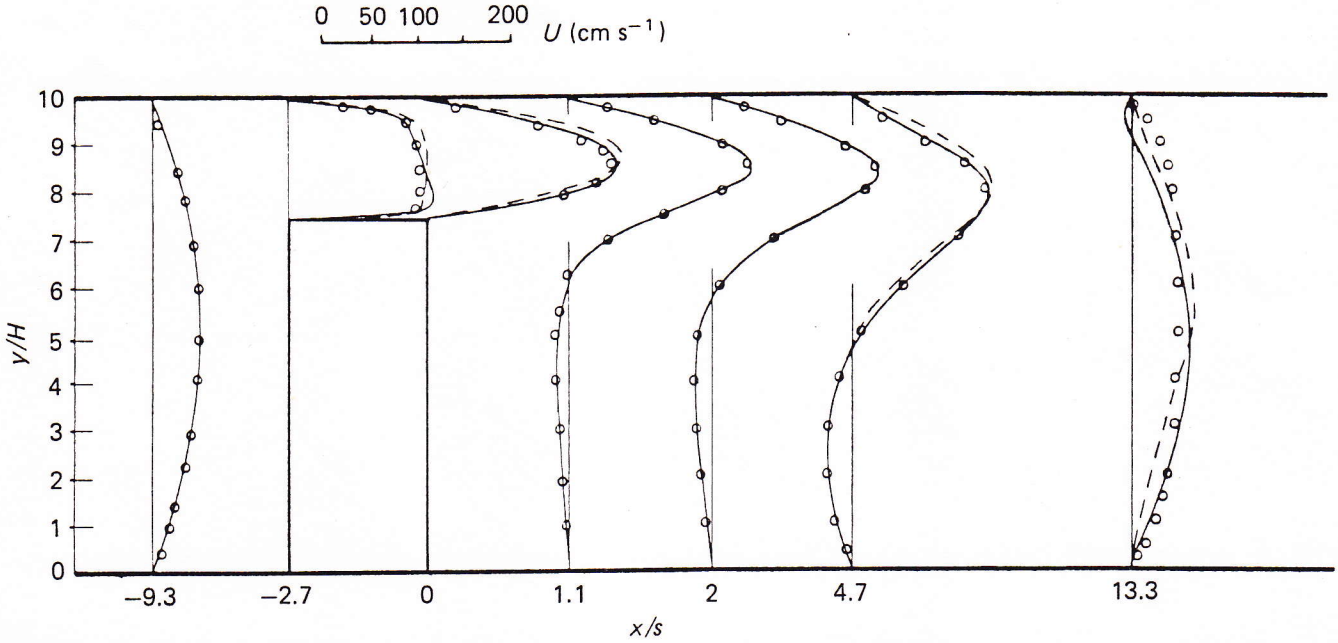

Figure 16 Comparison between predictions and measurements for flow over obstacle: $S/H = 0.75$; $Re_s = 177$; (——) CSUDS (38 × 35); (– – –) CUDS (69 × 53)

discrepancy only appears further downstream of the fence. Identical conclusions can be drawn from *Figures 13(a)* and *(b)* that illustrate the streamlines predicted with the QUDSC and the UDS schemes respectively.

High order schemes, such as QUDSC, proved to be difficult to handle when applied to flow over a fence or obstacle for Reynolds numbers higher than approximately 250. Problems in the solution arose with the fence with blockage ratio $S/H = 0.75$, for which 'wiggles' occurred in the solution of the predicted velocity fields, especially before the fence, in the region of steep velocity gradients, where the skewness of the flow is very strong. In this region, strong negative elements in the coefficient matrix arise simultaneously at several locations. The influence of these coefficients on the solution increases with Reynolds number Re_S (keeping the mesh distribution constant). It is worth noting that, with the 'wiggles', solutions up to $Re_S = 590$ could still be obtained. However, for $Re_S = 590$, the observed undershoots in the numerical solution of the flow field yielded a very small and unrealistic recirculation region before the fence and on the top channel wall.

Flow over an obstacle

The predictions carried out in this study of the flow over an obstacle were compared with experimental data provided by Gackstatter.[17] The geometrical flow configuration incorporated into the prediction is shown in *Figure 6* and the geometrical and flow parameters are listed in *Table 3*.

For a blockage ratio of $S/H = 0.25$, *Figure 14* shows the available experimental U-velocity profiles for $Re_S = 37$ and they are compared with predictions using the CSUDS and QUDSC schemes. The numerical calculation with the CSUDS and QUDSC schemes displays virtually coincident results. For one of the blockage ratios investigated, $S/H = 0.25$, the flow field is, from the point of view of flow predictions, simpler than the fence flow with the same blockage ratio (see *Table 2*, case I). The obstacle flow is similar to fence flow in the region of the front contraction. After this, the flow recovers above the obstacle to almost become a fully-developed channel flow. Hence, the downward flow results in a typical backward-facing step flow after the obstacle's rear surface, with the streamlines approaching the expansion cross-section nearly parallel.

Increasing the obstacle height to $S/H = 0.5$ increases the flow complexity. Nevertheless, even for this blockage ratio, no recirculation region was measured at the top wall,[13] nor was it predicted. It is this fact which makes the obstacle flow configuration less complicated in the downstream region in predicting laminar separated flows than the corresponding fence flow. *Figure 15* compares the measured U-velocity profiles with those calculated using the QUDSC and PLDS schemes for $Re_S = 96$. The QUDSC solution of the velocity field is in good agreement with the measurements, whilst the PLDS scheme shows a shorter recirculation region as a consequence of excessive false diffusion induced by the first order upwind scheme, at least in those flow regions where $|Pe| > 10$.

The last flow configuration investigated in this study was the flow over an obstacle with blockage ratio $S/H = 0.75$ and for $Re_S = 177$. *Figure 16* compares the CSUDS and CUDS schemes with the measured U-velocity. The high skewness and large velocity gradients of the flow before the obstacle may be the cause of numerical difficulties, resulting in strong simultaneous negative coefficients in the CSUDS scheme and producing over- and undershoots of the solutions. The fully developed channel flow, however, in establishing itself between the top obstacle surface and the top channel wall, prevents the downstream propagation of these under- or overshoots present in front of the obstacle. Although disagreements occurred between the CSUDS and CUDS schemes in the region $5 \leq X/S \leq 10$, the measured U-velocity data available are in relatively good

agreement with either the CSUDS or CUDS scheme predictions and measurements of the flow over a fence. The good agreement for $X/S<5$ may be explained by the fact that the high flow skewness is present together with very small velocities, and vice-versa. Numerically false diffusion, therefore, is very small in the flow field behind the rear step of the obstacle.

Conclusions

Flows over two-dimensional flow obstructions mounted in plane channel flow were predicted and compared with the measured velocity field. Two types of flow obstructions were compared, a fence and an elongated obstacle. For each of these obstructions, three blockage ratios of $S/H=0.25$, 0.5 and 0.75 were considered. In this way, the performance of five different numerical schemes for discretization of the convection terms in the basic fluid flow equations could be investigated for flow fields of different complexities. The schemes used in the present studies were the first order upwind (UDS), hybrid central/upwind (CUDS), hybrid power law/upwind (PLDS), hybrid central/skewed upwind (CSUDS) and quadratic upstream (QUDSC) schemes, the latter being corrected for non-uniform grids. For each of the six different flow geometries, a comparison between two of the aforementioned schemes was performed. This comparison demonstrated the superiority of the QUDSC and CSUDS schemes. The better performance of these schemes, in situations where convection is not primarily balanced by streamwise diffusion, is recognized and was demonstrated in this study.

Another conclusion that can be drawn from the present results is that, in many respects, flow over a fence is a more severe numerical test for the performance of the various schemes employed than the obstacle flow. In flow over a fence, numerical errors originating in front of the fence can be easily transmitted downstream and, hence, can influence predictions in the entire flow field. In contrast to this, flow over the obstacles used in this study, displays the characteristics of a backward-facing step type of flow, after the obstacle's rear surface. This part of the flow, in the absence of a recirculation region on the top channel wall, can be accurately predicted, even with low order finite difference schemes.

Although satisfactory predictions were obtained for most flows, the QUDSC scheme needs to be improved further in order to remove the over- or undershoots occurring in the flow predictions. The problem was detected for flow over a fence with a blockage ratio ≥ 0.75 and for $Re_S > 80$.

The present calculation clearly shows that the UDS, CUDS and PLDS schemes, in situations of strong coupling between transport processes in different directions, provide erroneous solutions. This behaviour is also present in the turbulent flow over fences and obstacles. Because of this, it should be concluded that, in order to investigate the validity of turbulent models in the flow geometries analysed in the present work, the UDS, CUDS and PLDS should be avoided, unless a very large computer storage is available and computer time is not severely limited.

In flow geometries with large regions where convection is primarily balanced by cross-stream diffusion or sources, the grid independence study for low order schemes should be based, in the absence of experimental data, on comparisons with results using higher order schemes or results using a numerical grid comprising high numbers of grid points, e.g. 150×100 or larger.

Acknowledgements

The present work was carried out with the support of the Deutsche Forschungsgemeinschaft within the DFG-Schwerpunktsprogramm: Finite Approximationen in der Strömungsmechanik. The authors gratefully acknowledge the support they have received for this work.

The completion of this work was aided by Dr Georg Scheuerer through useful and encouraging discussions. The final manuscript was completed with the help of Mrs B. Spinnler and Miss A. Messner.

References

1 Castro, I. P. 'The numerical prediction of recirculating flows', *Proc. 1st Int. Conf. Numer. Methods Laminar and Turbulent Flow, Swansea, Great Britain*, 1978, pp. 329–339

2 McGuirk, J. J., Taylor, A. M. K. P. and Whitelaw, J. H. 'The assessment of numerical diffusion in upwind-differencing calculations of turbulent recirculating flows', *Proc. Turbulent Shear Flows III*, Springer Verlag, 1985, 206–224

3 Leschziner, M. A. and Rodi, W. 'Calculation of annular and twin parallel jets using various discretisation schemes and turbulence model variations', *Trans. ASME*, 1981, **103**, 352–360

4 Roache, P. J. 'On artificial viscosity', *J. Comput. Phys.*, 1972, **10**(2), 351–366

5 Raithby, G. D. 'A critical evaluation of upstream differencing applied to problems involving fluid flow', *Comput. Meth. Appl. Mech. and Eng.*, 1976, **9**, 75–103

6 Leonard, B. P. 'A stable and accurate convective modelling procedure based on quadratic upstream interpolation', *Comput. Meth. Appl. Mech. and Eng.*, 1979, **19**, 59–98

7 Greenspan, D. 'Numerical studies of steady, viscous, incompressible flow in a channel with a step', *J. Eng. Math.*, 1969, (3), 21–28

8 Ghia, U. and Davis, R. I. 'Navier-Stokes solutions of flow past a class of two-dimensional semi-infinite bodies', *AIAA J.*, 1974, **12**(12), 1559–1665

9 Castro, I. P., Cliffe, K. A. and Norgett, M. J. 'Numerical predictions of the laminar flow over a normal flat plate', *Int. J. Numer. Meth. Fluids*, 1982, **2**, 62–88

10 Good, M. C. and Joubert, P. N. 'The drag of two-dimensional bulk plates immersed in turbulent boundary layers', *J. Fluid Mech.*, 1968, **31**, 547–582

11 Crabb, D., Durao, D. F. G. and Whitelaw, J. H. 'Velocity characteristics in the vicinity of a two-dimensional rib', *Proc. 4th Bras. Congr. of Mech. Eng.*, 1977, pp. 415–429

12 Durst, F. and Rastogi, A. K. 'Theoretical and experimental investigation of turbulent flow with separation' in 'Turbulent shear flow' Eds: F. Durst *et al.*, Springer Verlag, Berlin, 1980

13 Durst, F. and Founti, M. 'The wall reattaching flow over two-dimensional obstacles and preliminary scanning of the flow field with laser–Doppler anemometry', *LSTM-Erlangen Report 32/T/85, Universität Erlangen-Nürnberg*, 1984

14 Spalding, D. B. 'A novel finite difference formulation for differential expressions involving both first and second derivatives', *Int. J. Numer. Meth. Eng.*, 1972, **4**, 551–559

15 Patankar, S. V. 'Numerical heat transfer and fluid flow', Hemisphere Publishing, Washington, DC, 1980

16 Raithby, G. D. 'Skew upstream differencing schemes for problems involving fluid flow', *Comput. Meth. Appl. Mech. and Eng.*, 1976, **9**, 153–164

17 Gackstatter, R. 'Experimentelle Untersuchungen der abgelösten Strömung über zweidimensionale Hindernisse mittels Laser–Doppler-Anemometrie', *Diplomarbeit, LSTM-Erlangen, Universität Erlangen-Nürnberg*, 1984

18 Cherdon, W., Durst, F. and Whitelaw, J. H. 'Axisymmetric flows and instabilities in symmetric ducts with sudden expansions', *J. Fluid Mech.*, 1978, **84**, 13–31

19 Durst, F. and Tropea, C. 'Processing of laser–Doppler signals by means of a transient recorder and digital computer', *SFB 80/E/118 Rep., Sonderforschungsbereich 80, Universität Karlsruhe*, 1977

20 Armaly, B. F., Durst, F., Pereira, J. C. F. and Schönung, B. 'Experimental and theoretical investigations of backward-facing step flow', *J. Fluid Mech.*, 1983, **127**, 473–496

21 Durst, F. and Rastogi, A. K. 'Turbulent flow over two-dimensional fences', in 'Turbulent shear flow II' (eds J. S. Bradbury *et al.*), Springer Verlag, Berlin, 1980, pp. 218–232

22 Gosman, A. D. and Pun, W. M. Lecture notes for course entitled: 'Calculation of recirculating flows', *Rep. HTS/74/2, Dep. of Mech. Eng., Imperial College, London*, 1974

23 Durst, F. and Pereira, J. C. F. 'On the application of the quadratic upstream weighted scheme with non-uniform meshes', *LSTM-Erlangen Report 109/N/85, Universität Erlangen-Nürnberg*, 1985

24 Stone, H. L. 'Iterative solution of implicit approximations of multidimensional partial differential equations', *SIAM J. Numer. Anal.*, 1968, **5**(3), 530–558

25 Durst, F., Guggolz, M. G. and Pereira, J. C. F. 'Comparison of two methods for iterative solution of the approximated fluid flow equations', *LSTM-Erlangen Report 35/N/83, Universität Erlangen-Nürnberg*, 1983

26 Pereira, J. C. F. 'Experimentelle und Numerische Untersuchungen stationärer und instationärer Strömungen mit Ablösung', *Diss., Universität Erlangen-Nürnberg*, 1986

27 Zeisel, H. Erstellung einer Versuchs-einrichtung zur Untersuchung der Strömung über zweidimensionale Hindernisse mit einem LDA' Diplomarbeit, LSTM-Erlangen, Universität Erlangen-Nurnberg 1983

28 Dennis, S. C. R. and Smith, F. T. 'Steady flow through a channel with a symmetrical constriction in the form of a step', *Proc. R. Soc. London*, 1980, A.-372, pp. 393–414